J Biochem. 128, 57–64 (2000)

The Rate of Cell Growth Is Regulated by Purine Biosynthesis *via* ATP Production and G_1 to S Phase Transition[1]

Maki Kondo,* Takashi Yamaoka,†,2 Soichi Honda,* Yoshihiro Miwa,‡ Rumi Katashima,* Maki Moritani,* Katsuhiko Yoshimoto,* Yoshio Hayashi,‡ and Mitsuo Itakura†

**Otsuka Department of Molecular Nutrition, School of Medicine and ‡Dentistry, and †Division of Genetic Information, Institute for Genome Research, The University of Tokushima, Tokushima 770-8503*

Received March 10, 2000, accepted April 21, 2000

We recently showed that an increased supply of purine nucleotides increased the growth rate of cultured fibroblasts. To understand the mechanism of the growth rate regulation, CHO K1 (a wild type of Chinese hamster ovary fibroblast cell line) and CHO ade $^-$A (a cell line deficient in amidophosphoribosyltransferase, a rate-limiting enzyme of the *de novo* pathway) were cultured under various conditions. Moreover, a defective *de novo* pathway in CHO ade $^-$A cells was exogenously restored by 5-amino-4-imidazole-carboxamide riboside, a precursor of the *de novo* pathway. The following parameters were determined: the growth rate of CHO fibroblasts, the metabolic rate of the *de novo* pathway, the enzyme activities of amidophosphoribosyltransferase and hypoxanthine phosphoribosyltransferase, the content of intracellular nucleotides, and the duration of each cell-cycle phase. We concluded the following: (i) Purine *de novo* synthesis, rather than purine salvage synthesis or pyrimidine synthesis, limits the growth rate. (ii) Purine nucleotides are synthesized preferentially by the salvage pathway as long as hypoxanthine is available for energy conservation. (iii) The GTP content depends on the intracellular ATP content. (iv) Biosynthesis of purine nucleotides increases the growth rate mainly through ATP production and promotion of the G_1/S transition.

Key words: AICA riboside, ATP, cell cycle, growth rate, purine biosynthesis.

Supply of purine nucleotides through *de novo* and salvage pathways is essential for animal cell growth. In a previous study, we demonstrated that the activity of purine biosynthetic pathways, especially that of the *de novo* pathway, limits the growth rate of cultured fibroblasts (growth rate) (*1*), although the mechanism for this limitation was not fully understood. In this study, the mechanism by which purine nucleotides stimulate cell growth and shorten the doubling time was comprehensively examined. We used two cell lines: (i) CHO K1, a wild type of Chinese hamster ovary fibroblasts, and (ii) CHO ade $^-$A, an auxotrophic cell line deficient in amidophosphoribosyltransferase (ATase), which is a rate-limiting enzyme of the *de novo* pathway (*1*); and two kinds of culture media: (i) media rich in purine bases and (ii) media free of purine bases. In purine-rich media, both the *de novo* and salvage pathways function in CHO K1, but only the salvage pathway functions in CHO ade $^-$A. In purine-free media, only the *de novo* pathway functions in CHO K1, and neither pathway functions in CHO ade $^-$A. Furthermore, the *de novo* pathway of CHO ade $^-$A cells was restored by 5-amino-4-imidazole-carboxamide riboside (AICA riboside), a precursor for the *de novo* pathway, and exogenously controlled by the concentration of AICA riboside. Under various conditions, we determined several parameters including the growth rate of CHO fibroblasts, the metabolic rate of the *de novo* pathway, the enzyme activities of ATase and hypoxanthine phosporibosyltransferase (HPRT), the content of intracellular nucleotides, and the duration of each cell-cycle phase.

EXPERIMENTAL PROCEDURES

Cell Culture—CHO K1 and CHO ade $^-$A (*2*), which were kind gifts from Dr. David Patterson (Eleanor Roosevelt Institute for Cancer Research), were cultured at 37°C in an atmosphere of humidified air:CO_2 (95:5) in the following media: (I) Ham's F-12 (HamF) purine-rich medium containing 30 μM hypoxanthine (Hx) and 10% fetal calf serum (FCS); (II) HamF with 10% FCS treated with 1.25 mg (0.9 unit)/liter of xanthine oxidase (XO) from buttermilk (Sigma) at 37°C overnight, serving as a purine-free medium; (III) RPMI 1640 purine-free medium supplemented with 10% purine-free FCS. Purine bases in FCS were removed by dialysis at 4°C for 24 h (*1*). In media (I), both the *de novo* and salvage pathways function in CHO K1 cells, but only the salvage pathway functions in CHO ade $^-$A cells. In media (II) and (III), only the *de novo* pathway functions in CHO K1 cells, and neither pathway functions

[1] This study was supported in part by the Gout Research Foundation of Japan and the Otsuka Pharmaceutical Factory, Inc.

[2] To whom correspondence should be addressed Tel: +81-88-633-9483, Fax: +81-88-633-9484, E-mail: yamaoka@genome.tokushima-u.ac.jp

Abbreviations AICA riboside, 5-amino-4-imidazole-carboxamide riboside; ANOVA, analysis of variance; APRT, adenine phosphoribosyltransferase; ATase, amidophosphoribosyltransferase; CHO, Chinese hamster ovary, FCS, fetal calf serum, G_1/S transition, G_1 to S phase transition; HamF, Ham's F-12, HPRT, hypoxanthine phosphoribosyltransferase; Hx, hypoxanthine, *n*, sample number; *p*, probability; PBS, phosphate-buffered saline; PRPP, 5-phosphoribosyl 1-pyrophosphate; XO, xanthine oxidase.

in CHO ade⁻A cells. The complete removal of Hx in media (II) and (III) was confirmed firstly by the disappearance of the Hx peak in the reversed-phase high performance liquid chromatography analysis through a C18 column (*1*) and secondly by the lack of growth of CHO ade⁻A cells in these media. The *de novo* pathway in CHO ade⁻A cells functions only when AICA riboside (Sigma) is added to the medium.

Measurement of Growth Rate—Cultured cells during the logarithmic growth phase were counted with an improved Neubauer hemocytometer (*1*). The doubling time (h) was determined from cell counts and its reciprocal was defined as the growth rate.

Determination of Metabolic Rate of de Novo Pathway—The metabolic rate of the *de novo* pathway was determined by the incorporation of [^{14}C]formate (Amersham) into acid-soluble purines (*3*, *4*). In a 90-mm culture dish, 2×10^6 cells were plated. After the recovery of cell function from plating by 18 h of culture, [^{14}C]formate was added to the medium at the final concentration of 150 μM (0.3 MBq/ml). The cells were cultured in radioactive medium for 30 min, washed three times with 10 ml of ice-cold phosphate-buffered saline (PBS), and harvested with 1 ml of ice-cold perchloric acid (2 N) using a rubber policeman. After centrifugation at 12,000 ×*g* for 5 min at 4°C, the supernatant was heated at 100°C for 60 min, cooled on ice for 5 min, and applied to a column (0.5 × 3 cm) of AG-50W-X8 (Bio-Rad) equilibrated with 0.1 N HCl. After washing with 5 ml of 1 N HCl, the acid-soluble purines were eluted with 5 ml of 6 N HCl and counted with Aquasol-2 (Packard) in a scintillation counter.

Assay of ATase and HPRT Activities—Cell lysate for enzyme assay was prepared by sonication and centrifugation (*1*). To assay ATase activity, the cell lysate was incubated in 50 mM potassium phosphate buffer (pH 7.4) containing 5 mM 5-phosphoribosyl 1-pyrophosphate (Sigma; PRPP), 5 mM $MgCl_2$, 1 mM dithiothreitol, and 5 mM [^{14}C]glutamine (Amersham; 5.55 kBq/mmol) at 37°C for 1 h. The [^{14}C]-glutamate formed was separated from [^{14}C]glutamine by high-voltage paper electrophoresis at 800 W for 15 min and counted with toluene scintillation cocktail in a scintillation counter. The PRPP-dependent hydrolysis of glutamine to glutamate was regarded as representing ATase activity (*5*).

To assay HPRT activity, the cell lysate was incubated in 50 mM Tris-Cl (pH 7.4) containing 1.5 mM PRPP, 5 mM $MgCl_2$, and 5 mM [^{14}C]Hx (Amersham; 27.8 kBq/mmol) at 37°C for 20 min. The [^{14}C]IMP formed was separated from [^{14}C]Hx by high-voltage paper electrophoresis at 800 W for 15 min, and the [^{14}C]IMP spot on the filter paper was cut out under a UV lamp. The radioactivity of this spot was counted with toluene scintillation cocktail in a scintillation counter.

Determination of Intracellular Nucleotides—Cells in a 35-mm culture dish were lysed with 200 μl of 0.4 M perchloric acid, neutralized with 600 μl of 1 M Tris-Cl (pH 8.0), and centrifuged at 12,000 ×*g* for 5 min at 4°C. The supernatant was diluted with H_2O up to 10 ml, and 100 μl of the diluted sample was mixed with 100 μl of luciferase-luciferin reagent (ATP Bioluminescence Assay Kit HS II, Boehringer Mannheim). Luminescence from the reaction at room temperature was measured with a luminometer (Lumat LB9507, Berthold). The blank (no cells) was subtracted from the raw data, and the ATP concentration was determined from a log-log plot of the standard curve data. For GTP and GMP assays, nucleotides were extracted from cells with 0.7 M perchloric acid and neutralized with solid $KHCO_3$ (10 mg/100 μl) (*6*). The GTP and GMP peaks were detected with a UV monitor at 254 nm following HPLC on MonoQ HR5/5 column (Pharmacia) with a linear gradient from 20 mM to 1 M ammonium phosphate buffer (pH 7.0) for 60 min at a flow rate of 0.7 ml/min.

Cell Cycle Analysis with Flow Cytometric Methods—Cells in a 35-mm culture dish were detached with 0.1% trypsin and 0.02% EDTA and centrifuged at 500 ×*g* at 4°C for 5 min. The cell pellet was washed with 1 ml of PBS and fixed with 1 ml of 70% ethanol. After washing with 1 ml of PBS, fixed cells were incubated in 1 ml of PBS containing 0.1 mg/ml of RNase at 37°C for 1 h, then 50 μl of 2.5 mg/ml propidium iodide (Sigma) was added. Cell cycle analysis was performed with a flow cytometer (EPICS XL; Coulter). The duration of the individual phases of the cell cycle was estimated using the graphic method (*7*), which is based on the assumption that cells grow exponentially and asynchronously. The duration (h) of particular cell-cycle phases was calculated from the following formula: doubling time (h) × ln (1 + the fraction of cells in particular phases of the cell cycle).

Statistical Analysis—The data in Tables I and II are as means ± SE. For a comparison of two means, Student's paired or unpaired *t*-test was used. For a comparison of two groups, two-way analysis of variance (ANOVA) was used. The number (*n*) of samples for each point in all of the figures ranges from four to six. Because the SE of each point was small and amounted to less than 10% of the corresponding means, the representation of SE was omitted for clarity in all of the figures A probability value (*p*) of less than 0.05 was considered statistically significant.

RESULTS

Contribution of Purine and Pyrimidine Nucleotides to Growth Rate—To examine which nucleotide limits the growth rate, AICA riboside or uridine was added to medium in which CHO K1 cells were exponentially growing with sufficient nutrients (HamF) and 10% FCS. In animal cells, AICA riboside is converted to AICA riboside monophosphate by adenosine kinase, and then to IMP through the *de novo* pathway of purine nucleotides. Like AICA riboside, uridine is phosphorylated by uridine kinase and converted to UMP. At a concentration of 50 μM or less, AICA riboside increased the growth rate up to 20%, while uridine did not alter it at all (data not shown). This finding indicates that vigorously proliferating cells are prone to lack purine nucleotides and not pyrimidine nucleotides, *i.e.*, purine nucleotides limit the growth rate of cultured fibroblasts. At a concentration of more than 50 μM, AICA riboside decreased the growth rate (data not shown), because excessive AICA riboside inhibits pyrimidine biosynthesis (*8–10*).

Control of de Novo Pathway by AICA Riboside—To remove the effect of endogenous *de novo* and salvage pathways, CHO ade⁻A cells were arrested in a purine-free medium (HamF + 10% FCS + XO) for 48 h, then released from this purine-free arrest by AICA riboside administration. AICA riboside increased the metabolic rate of the *de novo* pathway in proportion to its concentration (Fig. 1): thus, we could exogenously regulate the metabolic rate of

the *de novo* pathway in CHO fibroblasts. When AICA riboside and uridine were used in combination, the metabolic rate of the *de novo* pathway increased by about 15% (Fig. 1).

Contribution of AICA Riboside to Growth Rate—CHO ade $^-$A cells arrested in a purine-free medium (HamF + 10% FCS + XO) for 48 h were stimulated by AICA riboside. The peak of the growth rate was shown at 50 μM AICA riboside concentration (Fig. 2). As in vigorously growing cells, AICA riboside at a concentration of more than 50 μM decreased the growth rate by inhibiting pyrimidine nucleotide biosynthesis (*8–10*). Uridine added in combination with AICA riboside compensated for the lack of pyrimidine nucleotides induced by excessive AICA riboside and further increased the growth rate (Fig. 2). AICA riboside and uridine were combined at various concentrations ranging from 0 to 1,000 μM and used to stimulate CHO ade $^-$A cells arrested in the purine-free medium (data not shown). The growth rate was maximized by the combination of 100 μM AICA riboside and 200 μM uridine (Fig. 2), which was therefore considered to maximize the contribution of the purine *de novo* pathway to the growth rate. The addition of uridine alone to arrested fibroblasts did not increase their growth rate.

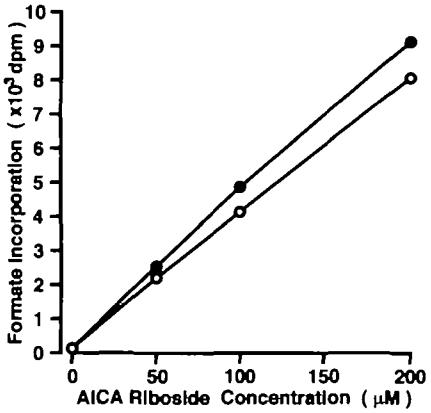

Fig 1 **Control of *de novo* pathway in CHO ade $^-$A cells by AICA riboside.** Formate incorporation indicates the metabolic rate of the *de novo* pathway CHO ade $^-$A cells arrested in HamF + 10% FCS + XO for 48 h were released by AICA riboside (○) and AICA riboside + 200 μM uridine (●) After the recovery of cell function by 18 h of culture, [^{14}C]formate was incorporated into purine nucleotides of CHO fibroblasts for 30 min Formate incorporation was higher when AICA riboside was added with uridine than that without uridine ($p < 0.05$, by two-way ANOVA)

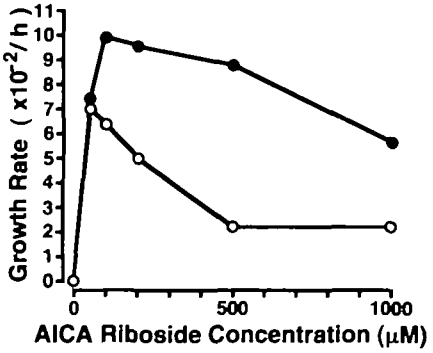

Fig. 2. **Increase in the growth rate of CHO ade $^-$A cells by AICA riboside.** CHO ade $^-$A cells arrested in HamF + 10% FCS + XO for 48 h were released by AICA riboside (○) and AICA riboside + 200 μM uridine (●). Proliferating cells during the logarithmic growth phase were counted every 24 h, and the growth rate was determined.

Contribution of Purine Bases to Growth Rate—CHO ade $^-$A cells in a purine-free medium (RPMI1640 + 10% dialyzed FCS) were released from growth arrest for 48 h by supplementation with purine bases at various concentrations. Hx increased the growth rate more effectively than adenine, while no cell growth was observed with guanine as the only source of the salvage pathway (Fig. 3). The maximal growth rate was attained with Hx at a concentration of more than 30 μM. It was, therefore, considered that Hx at a concentration over 30 μM drives the growth through the salvage pathway at its maximum in CHO ade $^-$A fibroblasts. These observations demonstrated that Hx is the principal source for the salvage pathway in CHO ade $^-$A fibroblasts. The growth rate found with 30 μM Hx did not increase even when uridine was also added to the 30 μM Hx.

Increase in Growth Rate by de Novo and Salvage Pathways—The growth rate of CHO ade $^-$A cells was measured when the *de novo* and salvage pathways of the cells in the purine-free media (HamF + 1% or 10% FCS + XO) were activated at their maximum by 100 μM AICA riboside + 200 μM uridine and 30 μM Hx, respectively. The growth

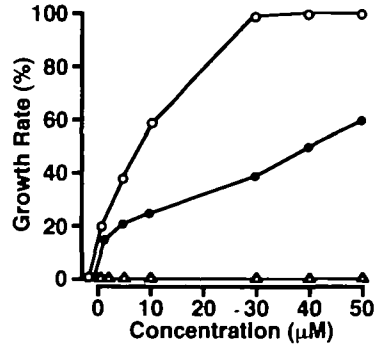

Fig 3 **Increase in the growth rate of CHO ade $^-$A cells by purine bases.** *CHO ade $^-$A cells arrested in RPMI1640 + 10% dialyzed FCS for 48 h were released by Hx (○), adenine (●), and guanine (△). Proliferating cells during the logarithmic growth phase were counted every 24 h, and the growth rate was determined The maximal growth rate with Hx is represented as 100%.*

TABLE I **Contribution of purine biosynthetic pathway(s) to increase in growth rate.**

Functioning purine biosynthetic pathway(s)	Growth rate (×10^{-2}/h)	
	1% FCS	10% FCS
De novo[a] (*n*=6)	8.6 ± 0.2 *	8.8 ± 0.1 **
Salvage[b] (*n*=6)	7.5 ± 0.3 *	8.0 ± 0.1 **
De novo & salvage[c] (*n*=6)	8.6 ± 0.3	8.8 ± 0.1

CHO ade $^-$A cells arrested in HamF + 1% or 10% FCS + XO for 48 h were released by 100 μM AICA riboside + 200 μM uridine (a), 30 μM Hx (b), and 100 μM AICA riboside + 200 μM uridine + 30 μM Hx (c) Proliferating cells during the logarithmic growth phase were counted every 24 h, and the growth rate was determined. *$p < 0.05$, **$p < 0.01$

rate when only the *de novo* pathway was functioning was significantly higher than that when only the salvage pathway was functioning (Table I). Furthermore, the growth rate when only the *de novo* pathway was functioning was comparable to that when both pathways were functioning, irrespective of FCS concentration (Table I).

Cell-Cycle Analysis of ATase and HPRT—ATase and HPRT are key enzymes of the *de novo* and salvage pathways, respectively. To examine when each pathway is activated in the phases of the cell cycle, the cell-cycle-dependent expression of ATase and HPRT was examined. CHO K1 cells (1×10^6 cells/90-mm culture dish) were synchronized in the G_0/G_1 phase by serum deprivation (HamF + 0.1% FCS) for 48 h, and released with 10% FCS (*11*). In flow cytometric analysis, the G_1 to S phase transition (G_1/S transition) started 6 h after stimulation by 10% FCS (Fig. 5A), and ATase activity was elevated at the maximal plateau level by 6 h (Fig. 4). These results indicate that ATase expression increases from the late G_1 phase to the S phase, whereas HPRT activity is nearly constant during the cell cycle (Fig. 4), suggesting that the *de novo* pathway is more important than the salvage pathway for supplying purine nucleotides in proliferating fibroblasts. When CHO ade$^-$A cells arrested by serum starvation were cultured with AICA riboside or uridine, no growth occurred.

Recovery of CHO ade$^-$A Cells from Purine-Free Arrest—CHO ade$^-$A cells were arrested in the purine-free media (HamF + 10% FCS + XO) for 48 h, and flow cytometric analysis revealed that a complete shutdown of both biosynthetic pathways of purine nucleotides causes CHO ade$^-$A cells to accumulate in the G_0/G_1 phase. Arrested fibroblasts were released by 100 μM AICA riboside, 100 μM AICA riboside + 200 μM uridine, 30 μM Hx, or 100 μM AICA riboside + 200 μM uridine + 30 μM Hx, and the time (h) to the G_1/S transition was measured. When only the *de novo* pathway was functioning (AICA riboside or AICA riboside + uridine), the G_1/S transition started from 12 h after the release from the cell-cycle arrest (Fig. 5B). When only the salvage pathway was functioning (Hx), and when both pathways were functioning (AICA + uridine + Hx), CHO ade$^-$A cells in the G_1 phase started to enter the S phase after 6 h (Fig. 5, C and D).

Determination of Intracellular Nucleotides—The G_1/S transition by release from purine-free arrest occurred earlier when the salvage pathway was functioning (Fig. 5C) than when the *de novo* pathway was active (Fig. 5B), which is explained by the difference of ATP consumption in these two pathways. The *de novo* pathway and the conversion of AICA riboside and uridine to AICA ribotide and UMP, respectively, need an ATP supply, whereas the salvage pathway does not. Therefore, intracellular ATP content was assayed.

First, the change in intracellular ATP was examined during release from purine-free arrest (Fig. 6). Purine-free arrest decreased the intracellular ATP content to about 10% of its normal level (7–10 nmol/10^6 cells). Recovery from ATP depletion was earlier when only the salvage pathway was functioning (HamF) than when only the *de novo* pathway was functioning (HamF + XO + 100 μM AICA riboside with or without 200 μM uridine). Furthermore, the increase in ATP content due to the salvage pathway alone (HamF) was comparable to that produced by both the *de novo* and salvage pathways (HamF + 100 μM AICA riboside + 200 μM uridine). These findings indicate that the

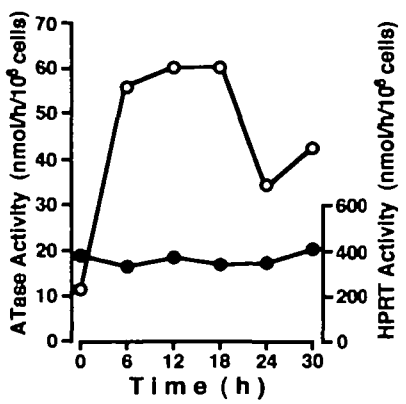

Fig. 4. **Cell-cycle-dependent change of ATase and HPRT activities.** CHO K1 cells were synchronized in HamF + 0.1% FCS for 48 h. After stimulation by 10% FCS, ATase (○) and HPRT (●) activities were assayed every 6 h up to 30 h.

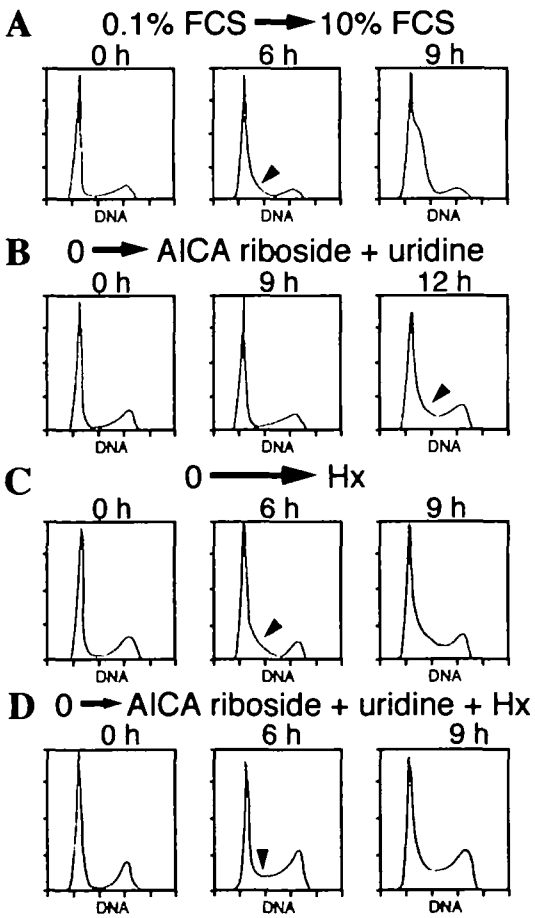

Fig. 5 **Flow cytometric analysis.** The times from the release from growth arrest to the G_1/S transition were measured. Arrowheads indicate the start of the G_1/S transition. A. Recovery from serum starvation. CHO K1 cells synchronized in HamF + 0.1% FCS for 48 h were stimulated by 10% FCS. B–D. Recovery from purine-free arrest through the *de novo* pathway (B), the salvage pathway (C), and both pathways (D). CHO ade$^-$A cells arrested in HamF + 10% FCS + XO for 48 h were released by 100 μM AICA riboside (B), 30 μM Hx (C), and 100 μM AICA riboside + 200 μM uridine + 30 μM Hx (D).

salvage pathway increases the intracellular ATP content more efficiently than the *de novo* pathway when purine nucleotides are depleted, which would explain why the salvage pathway (Fig. 5C) leads to the earlier G_1/S transition from purine-free arrest than does the *de novo* pathway (Fig. 5B).

Secondly, the effect of purine bases, substrates for the salvage pathway, on intracellular ATP content was examined (Fig. 7). Hx increased the ATP content of CHO ade⁻A cells arrested in purine-free medium more than adenine, whereas guanine hardly increased the intracellular ATP content. These results are consistent with the effect of each purine base on the growth rate (Fig. 3). Hx and adenine also increased the GTP content with ATP, whereas guanine increased neither the ATP nor the GTP content (Fig. 7), although the GMP content increased from 21.1 ± 1.9 to 39.0 ± 3.1 pmol/10^6 cells due to guanine administration. These results suggest that the GTP content depends on the ATP content, *i.e.*, phosphorylation of GMP and GDP by ATP.

Duration of Individual Cell-Cycle Phases—Supplying purine nucleotides mainly shortened the duration of the G_1 phase, and the S phase was also shortened to a small degree (Table II). The contribution of the *de novo* pathway (CHO K1 cells in HamF + XO) to the shortening of the G_1 phase was larger than that of the salvage pathway (CHO ade⁻A in HamF), which is consistent with the result that the *de novo* pathway of CHO ade⁻A cells activated by AICA riboside increased the growth rate more than the salvage pathway with Hx (Table I).

DISCUSSION

Contribution of Purine and Pyrimidine Nucleotides to Growth Rate—In this study, the addition of uridine increased the growth rate only in the case of pyrimidine deprivation by AICA riboside. AICA riboside increased the growth rate of exponentially proliferating CHO K1 cells, while uridine did not. However, AICA riboside did not release CHO K1 cells from cell-cycle arrest by serum starvation. These results indicate that purine nucleotides limit the growth rate of cultured fibroblasts under the stimulation of growth factors in FCS. Indeed, DNA replication in nuclei isolated from murine myeloid cells did not start even in the presence of sufficient NTPs and dNTPs without stimulation of cell growth by interleukin-3 (*12*).

Control of de Novo Pathway by AICA Riboside—The increase in the metabolic rate of the *de novo* pathway by AICA riboside was enhanced by uridine (Fig. 1). This effect of uridine is explained as follows: An insufficiency of pyrimidine nucleotides induced by excessive AICA riboside was restored by uridine, and the improved balance of purine and pyrimidine nucleotides increased RNA and DNA syntheses, resulting in increases in consumption and the *de novo* synthesis of purine nucleotides. Pyrimidine starvation by AICA riboside is regarded, at least in part, as a result of PRPP depletion by conversion of AICA riboside monophos-

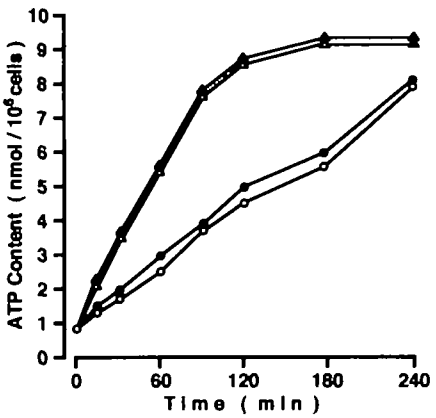

Fig. 6. **Recovery from ATP depletion.** CHO ade⁻A cells arrested in HamF + 10% FCS + XO for 48 h were released by HamF + 10% FCS + XO + 100 μM AICA riboside (○; only the *de novo* pathway functions), HamF + 10% FCS + XO +100 μM AICA riboside + 200 μM uridine (●; only the *de novo* pathway functions), HamF + 10% FCS (△; only the salvage pathway functions), or HamF + 10% FCS + 100 μM AICA riboside + 200 μM uridine (▲; both pathways function).

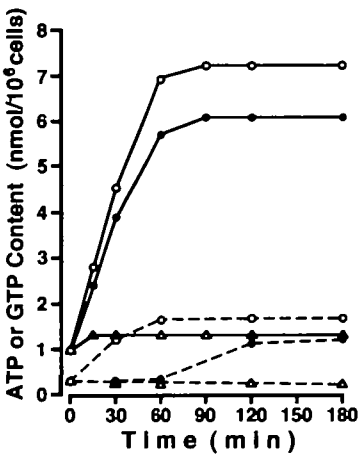

Fig. 7. **Recovery from nucleotide depletion by purine bases.** CHO ade⁻A cells arrested in RPMI1640 + 10% dialyzed FCS for 48 h were released by 30 μM Hx (○), 30 μM adenine (●), or 30 μM guanine (△). Solid and dashed lines indicate ATP and GTP content, respectively.

TABLE II. **Effect of purine biosynthetic pathway(s) on duration of cell-cycle phases.**

Cell	Medium	G_1	S	G_2/M	Doubling time (h)
CHOK1 (n=4)	HamF	2.3 ± 0.1	3.2 ± 0.2	4.8 ± 0.2	10.3[a]
CHOK1 (n=4)	HamF+XO	3.0 ± 0.3 **	3.0 ± 0.4 *	5.0 ± 0.3	11.0[b]
CHO ade⁻A (n=4)	HamF	5.8 ± 0.3 **	4.6 ± 0.3 *	4.8 ± 0.3	15.3[c]

The duration of the individual phases of the cell cycle was determined using the graphic method (*7*). [a]Both the *de novo* and salvage pathways are functioning. [b]Only the *de novo* pathway is functioning. [c]Only the salvage pathway is functioning. *$p < 0.05$; **$p < 0.01$.

phate to AICA riboside triphosphate (*8–10*). Moreover, the accumulation of intracellular AICA riboside monophosphate was reported to inhibit adenylosuccinate lyase and the subsequent synthesis of ATP (*13*). However, the accumulation of AICA riboside monophosphate in CHO fibroblasts was negligible when AICA riboside was used at a concentration of less than 150 μM, and the predominant metabolic fate of AICA riboside is IMP (*14*). IMP produced from AICA riboside at relatively low concentrations enters the adenylate and guanylate pools, and proportionally increases intracellular ATP and GTP (*10*, *14*, *15*).

Contribution of Purine Bases to Growth Rate—Hx is converted to IMP *via* the catalysis of HPRT, and subsequently to GMP and AMP in proper proportions. Although adenine and guanine are converted to AMP and GMP, respectively, by adenine phosphoribosyltransferase (APRT) and HPRT, respectively, the inter-conversion between AMP and GMP does not occur at the level of nucleotides in mammalian fibroblasts (*15*, *16*). Indeed, guanine hardly increased the intracellular ATP content (Fig. 7), leading to no cell growth (Fig. 3). Therefore, Hx and HPRT are, in general, the most important source and enzyme, respectively, of the salvage pathway. In contrast to guanine, adenine increased ATP with GTP (Fig 7) and the growth rate of CHO ade⁻A cells (Fig. 3) without purine supply *via* the *de novo* pathway, indicating that the adenine rather than guanine nucleotide pool limits the growth rate. Because adenine increased the GTP content after repletion of the ATP content (Fig. 7), GTP production from adenine in fibroblasts is explained as follows: Adenine is salvaged by APRT to form AMP. After ATP repletion by phosphorylation of AMP, excessive AMP is catabolized to Hx. Hx is salvaged by HPRT to form IMP. IMP is converted to AMP and GMP. GMP is phosphorylated by ATP to form GTP. This mechanism (*17*) may function to prevent an imbalance of purine nucleotides by excessive adenine nucleotides even under physiological conditions. Furthermore, it was indirectly demonstrated that AMP is not catabolized until the ATP pool is filled. In contrast to AMP, excessive GMP is catabolized to xanthine, not Hx. Therefore, IMP is not produced from GMP catabolites, resulting in no ATP production (Fig. 7).

Contributions of de Novo and Salvage Pathways to Growth Rate—Both the *de novo* pathway of CHO ade⁻A cells exogenously activated by AICA riboside (Table I) and the endogenous *de novo* pathway in CHO K1 cells (Table II) increased the growth rate, *i.e.*, shortened the cell doubling time, more than the salvage pathway. The importance of the *de novo* pathway for cell growth was also shown by the cell-cycle-dependent expression of ATase (Figs. 4 and 5A). In contrast to constant expression of HPRT, ATase expression increased from the late G_1 to the S phase. This ATase probably supplies the source of RNA, DNA, and ATP syntheses for cell division. The expression of ATase mRNA also increased to its maximal level at the G_1/S boundary (Honda, S., Kondo, M., Yamaoka, T., and Itakura, M., unpublished observation).

In the rat hepatocyte cell line, the basal activities of the enzymes of the *de novo* pathway were 1.7 to 6.8 times higher than in normal rat liver, whereas those of the purine salvage enzymes were unchanged. Furthermore, the activities of purine *de novo* synthetic enzymes increased by a factor of 1.3 to 2.4 in the log phase compared to the plateau phase, but those of the salvage enzymes were unchanged (*18*). In human T lymphocytes, *de novo* purine biosynthetic activity was found only in large S-phase thymocytes, whereas both G_1-phase small thymocytes and peripheral blood T lymphocytes lacked any significant activity (*19*). Thus resting T lymphocytes meet their metabolic demands *via* the salvage pathway, while intact *de novo* synthesis is essential for the proliferation of phetohemagglutinin-stimulated T lymphocytes (*20*). Even in patients with Lesch-Nyhan syndrome, where the salvage pathway by HPRT does not function, the proliferation of T lymphocytes in response to mitogenic or antigenic stimulation is normal (*21*) due to compensation of accelerated *de novo* synthesis (*22*).

Changes of Intracellular Nucleotide Content—In this study, we first demonstrated without metabolic inhibitors that the complete shutdown of both biosynthetic pathways of purine nucleotides decreases intracellular ATP content to 10% (Fig. 6) and leads to cell arrest in the G_0/G_1 phase (Fig. 5, B–D). The recovery of intracellular ATP content from purine-free arrest by the salvage pathway alone was comparable to that by both the *de novo* and salvage pathways (Fig. 6), indicating that the *de novo* pathway makes no additional contribution to ATP production in the presence of the salvage pathway. This is consistent with the concept that purine nucleotides are synthesized preferentially by the salvage pathway as long as Hx is available, with the concomitant suppression of the *de novo* pathway, which spares the energy expenditure required for *de novo* synthesis (*1*).

In this study, strong links were found among the purine biosynthetic activity, the intracellular ATP content, the timing of the G_1/S transition, the shortening of the G_1-phase duration, and the growth rate. Firstly, the early increase of ATP by the salvage pathway (Fig. 6) led to the early G_1/S transition (Fig. 5C). Secondly, the ability of purine bases to produce ATP (Fig. 7) was strongly associated with their ability to increase the growth rate (Fig. 3). Thirdly, purine biosynthesis mainly shortened the duration of the G_1 phase, *i.e.*, hastened the G_1/S transition, leading to the decrease in doubling time and the increase in the growth rate (Table II). These results strongly suggest that the biosynthesis of purine nucleotides increases the growth rate through the production and concentration of ATP and promotion of the G_1/S transition. Indeed, the intracellular ATP content in fibroblasts increased (*23*) from 3.3 nmol/10^6 cells in the G_1 phase to 8.2 nmol/10^6 cells by the early S phase (*24*), and it seems that growing cells have the threshold intracellular ATP concentration necessary for passage at the G_1/S checkpoint (*25*, *26*). It is not fully understood how increased ATP in the late G_1 phase promotes the G_1/S transition. In growing lambs, 19 and 39% of whole-body ATP are used for protein turnover and Na^+,K^+-transport, respectively (*27*). Both in bacteria (*28*) and mammalian cells (*29*), the concentrations of ATP and GTP control rRNA transcription, which is the rate-limiting step of ribosome synthesis for protein synthesis. Activation (*30*) and inhibition (*31*) of ATP-sensitive K^+ channels were reported to lead to the G_1/S transition and the G_0/G_1 arrest, respectively. ATP is also necessary for DNA topoisomerase II, which increases in the late G_1 phase (*32*) and is essential for the G_1/S transition (*33*). Moreover, ATP regulates cyclin/cyclin-dependent kinase complexes for the G_1/S transition (*34*).

Biosynthesis of purine nucleotides shortened not only the G_1-phase duration, but also the S-phase duration to a small degree (Table II). Because the pool size of pyrimidine dNTPs was about 5–10 times greater than that of purine dNTPs in mouse fibroblasts (*23*, *24*), and because RNA primers for the initiation of DNA synthesis always begin with A or G (*35*), purine nucleotide probably limits the rate of DNA replication, as well as the G_1/S transition.

No effect of purine biosynthesis on the duration of the G_2/M phase was observed. However, purine-free arrest may also occur at the G_2/M checkpoint in addition to the G_1/S checkpoint, because a modest accumulation of CHO ade$^-$A cells was observed at the G_2/M peak in purine-free medium (Fig. 5, B–D). Indeed, severe ATP depletion by the disruption of mitochondrial function resulted in G_2/M arrest in addition to G_1 arrest (*25*). Moreover, intracellular ATP content increases from 4.0 nmol/10^6 cells during the late S phase to 6.6 nmol/10^6 cells with the onset of cell division, which is the second peak of intracellular ATP after the first peak during G_1/S transition (*24*). Growing cells may have a threshold intracellular ATP concentration for passage at the G_2/M checkpoint, as well as the putative ATP threshold at the G_1/S checkpoint.

For ATP production, several factors are necessary including sufficient nutrients such as glucose (*36*, *37*), oxygen (*38*) with electron transport in mitochondria (*37*), and biosynthesis of adenine nucleotides through the *de novo* and salvage pathways. In this study, even with sufficient nutrients and oxygen, the intracellular ATP content decreased to 10% when the two purine synthetic pathways were completely shut down. This indicates the importance of purine biosynthesis for ATP production, as well as phosphorylation of ADP *via* glycolysis or electron transport. In contrast to ATP, GTP is chiefly produced by phosphorylation of GDP by ATP, as well as other NTPs and dNTPs. Therefore, GTP production is under the control of ATP (Fig. 7), and ATP is considered to be the most important nucleotide for supply of NTPs and dNTPs for cell growth. GTP also plays an important role in cell growth: for example, signal transduction of small GTPases such as Ras, Rho, and Ran. However, the pool size of GTP is maintained by ATP at a nearly constant level sufficient for cell growth throughout the cell cycle (*24*).

In conclusion, the following concepts were supported in this study using CHO fibroblasts. Firstly, purine *de novo* synthesis, rather than purine salvage synthesis or pyrimidine synthesis, limits the growth rate. Secondly, purine nucleotides are synthesized preferentially by the salvage pathway as long as Hx is available for energy conservation. Thirdly, the GTP content depends on the ATP content. Lastly, biosynthesis of purine nucleotides increases the growth rate mainly through ATP production and promotion of the G_1/S transition. Understanding the mechanism by which purine biosynthesis increases ATP and the growth rate is very useful for developing therapies for malignant neoplasms (*39*) and for ischemic diseases including brain (*38*) and myocardial (*40*) infarctions.

REFERENCES

1. Yamaoka, T., Kondo, M., Honda, S., Iwahana, H., Moritani, M., Ii, S., Yoshimoto, K., and Itakura, M. (1997) Amidophosphoribosyltransferase limits the rate of cell growth-linked *de novo* purine biosynthesis in the presence of constant capacity of salvage purine biosynthesis. *J. Biol. Chem.* **272**, 17719–17725
2. Oates, D.C. and Patterson, D. (1977) Biochemical genetics of Chinese hamster cell mutants with deviant purine metabolism: characterization of Chinese hamster cell mutants defective in phosphoribosylpyrophosphate amidotransferase and phosphoribosylglycinamide synthetase and an examination of alternatives to the first step of purine biosynthesis. *Somatic Cell Genet.* **3**, 561–577
3. Tsuchiya, M., Yoshikawa, H., Itakura, M., and Yamashita, K. (1990) Increased *de novo* purine synthesis by insulin through selective enzyme induction in primary cultured rat hepatocytes. *Am. J. Physiol.* **258**, C841–848
4. Boss, G.R. and Erbe, R.W. (1982) Decreased purine synthesis during amino acid starvation of human lymphoblasts. *J. Biol. Chem.* **257**, 4242–4247
5. Itakura, M. and Holmes, E.W. (1979) Human amidophosphoribosyltransferase. An oxygen-sensitive iron-sulfur protein. *J. Biol. Chem.* **333**, 999–1003
6. Kremmer, T., Paulik, E., Boldizsar, M., and Holenyi, I. (1989) Application of the fast protein liquid chromatographic system and MonoQ HR 5/5 anion exchanger to the separation of nucleotides. *J. Chromatogr.* **493**, 45–52
7. Okada, S. (1967) A simple graphic method of computing the parameters of the life cycle of cultured mammalian cells in the exponential growth phase. *J. Cell Biol.* **34**, 915–916
8. Thomas, C.B., Meade, J.C., and Holmes, E.W. (1981) Aminoimidazole carboxamide ribonucleoside toxicity: a model for study of pyrimidine starvation. *J. Cell. Physiol.* **107**, 335–344
9. Sabina, R.L., Holmes, E.W., and Becker, M.A. (1984) The enzymatic synthesis of 5-amino-4-imidazolecarboxamide riboside triphosphate (ZTP). *Science* **223**, 1193–1195
10. Gong, Y.F., Srinivas, R.V., and Fridland, A. (1993) 5-Amino-4-imidazolecarboxamide riboside potentiates the metabolism and anti-human immunodeficiency virus activity of 2',3'-dideoxyinosine. *Mol. Pharmacol.* **44**, 30–36
11. Fantes, P. and Brooks, R. (1993) *The Cell Cycle: A Practical Approach*, IRL Press, New York
12. Munshi, N.C. and Gabig, T.G. (1990) Growth factor-dependent initiation of DNA replication in nuclei isolated from an interleukin 3-dependent murine myeloid cell line. *J. Clin. Invest.* **85**, 300–304
13. Sabina, R.L., Kernstine, K.H., Boyd, R.L., Holmes, E.W., and Swain, J.L. (1982) Metabolism of 5-amino-4-imidazolecarboxamide riboside in cardiac and skeletal muscle. Effects on purine nucleotide synthesis. *J. Biol. Chem.* **257**, 10178–10183
14. Sabina, R.L., Patterson, D., and Holmes, E.W. (1985) 5-Amino-4-imidazolecarboxamide riboside (Z-riboside) metabolism in eukaryotic cells. *J. Biol. Chem.* **260**, 6107–6114
15. Page, T. (1989) Purine nucleotide production in normal and HPRT-cells. *Int. J. Biochem.* **21**, 1377–1381
16. Zoref-Shani, E. and Sperling, O. (1980) Characterization of purine nucleotide metabolism in cultured fibroblasts with deficiency of hypoxanthine-guanine phosphoribosyltransferase and with superactivity of phosphoribosylpyrophosphate synthetase. *Enzyme* **25**, 413–418
17. Becker, M.A., Kim, M., Husain, K., and Kang, T. (1992) Regulation of purine nucleotide synthesis in human B lymphoblasts with both hypoxanthine-guanine phosphoribosyltransferase deficiency and phosphoribosylpyrophosphate synthetase superactivity. *J. Biol. Chem.* **267**, 4317–4321
18. Mayer, D., Natsumeda, Y., Ikegami, T., Faderan, M., Lui, M., Emrani, J., Reardon, M., Olah, E., and Weber, G. (1990) Expression of key enzymes of purine and pyrimidine metabolism in a hepatocyte-derived cell line at different phases of the growth cycle. *J. Cancer Res. Clin. Oncol.* **116**, 251–258
19. Cohen, A., Barankiewicz, J., Lederman, H.M., and Gelfand, E.W. (1984) Purine metabolism in human T lymphocytes: role of the purine nucleoside cycle. *Can. J. Biochem. Cell Biol.* **62**, 577–583
20. Fairbanks, L.D., Bofill, M., Ruchemmann, K., and Simmonds, H.A. (1995) Importance of ribonucleotide availability to prolif-

erating T-lymphocytes from healthy humans. Disproportionate expansion of pyrimidine pools and contrasting effects of *de novo* synthesis inhibitors. *J. Biol Chem.* **270**, 29682–29689
21 Allison, A.C., Hovi, T., Watts, R.W, and Webster, A.D (1975) Immunological observations on patients with Lesch-Nyhan syndrome, and on the role of *de novo* purine synthesis in lymphocyte transformation. *Lancet* **7946**, 1179–1183
22. Brosh, S., Boer, P., Kupfer, B., deVries, A., and Sperling, O (1976) *De novo* synthesis of purine nucleotides in human peripheral blood leukocytes. Excessive activity of the pathway in hypoxanthine-guanine phosphoribosyltransferase deficiency. *J Clin. Invest.* **58**, 289–297
23. Hordern, J. and Henderson, J.F. (1982) Comparison of purine and pyrimidine metabolism in G_1 and S phases of HeLa and Chinese hamster ovary cells. *Can. J. Biochem.* **60**, 422–433
24 McCormick, P.J., Danhauser, L.L., Rustum, Y.M, and Bertram, J.S. (1983) Changes in ribo- and deoxyribonucleoside triphosphate pools within the cell cycle of a synchronized mouse fibroblast cell line. *Biochim Biophys. Acta* **756**, 36–40
25. Sweet, S and Singh, G (1995) Accumulation of human promyelocytic leukemic (HL-60) cells at two energetic cell cycle checkpoints. *Cancer Res.* **55**, 5164–5167
26. Zhang, C.C., Boritzki, T.J, and Jackson, R.C. (1998) An inhibitor of glycinamide ribonucleotide formyltransferase is selectively cytotoxic to cells that lack a functional G_1 checkpoint. *Cancer Chemother. Pharmacol* **41**, 223–228
27. Gill, M, France, J., Summers, M., McBride, B.W., and Milligan, L.P (1989) Simulation of the energy costs associated with protein turnover and Na^+,K^+-transport in growing lambs. *J. Nutr* **119**, 1287–1299
28. Gaal, T, Bartlett, M.S., Ross, W., Turnbough Jr., C.L., and Gourse, R.L. (1997) Transcription regulation by initiating NTP concentration rRNA synthesis in bacteria *Science* **278**, 2092–2097
29. Grummt, I and Grummt, F (1976) Control of nucleolar RNA synthesis by the intracellular pool sizes of ATP and GTP *Cell* **7**, 447–453
30. Strobl, S.J, Wonderlin, W.F, and Flynn, D.C. (1995) Mitogenic signal transduction in human breast cancer cells. *Gen. Pharmacol* **26**, 1643–1649
31 Woodfork, K.A., Wonderlin, W.F., Peterson, V.A., and Strobl, J.S. (1995) Inhibition of ATP-sensitive potassium channels causes reversible cell-cycle arrest of human breast cancer cells in tissue culture. *J Cell. Physiol.* **162**, 163–171
32 Epstein, R.J and Smith, P.J (1989) Mitogen-induced topoisomerase II synthesis precedes DNA synthesis in human breast cancer cells. *Biochem. Biophys. Res. Commun.* **160**, 12–17
33. Rappa, G, Lorico, A., and Sartorelli, A.C. (1992) Development and characterization of a WEHI-3B D+ monomyelocytic leukemia cell line resistant to novobiocin and cross-resistant to other topoisomerase II-targeted drugs. *Cancer Res.* **52**, 2782–2790
34. Sheaff, R.J., Groudine, M., Gordon, M., Roberts, J.M., and Clurman, B.E. (1997) Cyclin E-CDK2 is a regulator of p27Kip1 *Genes Dev.* **11**, 1464–1478
35. Yamaguchi, M., Hendrickson, E.A., and DePamphilis, M.L. (1985) DNA primase-DNA polymerase alpha from simian cells. Modulation of RNA primer synthesis by ribonucleoside triphosphates. *J Biol Chem.* **260**, 6254–6263
36. Lazo, P.A. (1981) Amino acids and glucose utilization by different metabolic pathways in ascites-tumour cells. *Eur. J Biochem* **117**, 19–25
37. Zoref-Shani, E., Kessler-Icekson, G, and Sperling, O. (1988) Pathways of adenine nucleotide catabolism in primary rat cardiomyocyte cultures. *J. Mol Cell Cardiol.* **20**, 23–33
38 Pissarek, M., Reichelt, C, Krauss, G.J., and Illes, P. (1998) Tolbutamide attenuates diazoxide-induced aggravation of hypoxic cell injury. *Brain Res.* **812**, 164–171
39. Smith, J.L., Zaluzec, E.J., Wery, J.P., Niu, L., Switzer, R.L, Zalkin, H, and Satow, Y (1994) Structure of the allosteric regulatory enzyme of purine biosynthesis. *Science* **264**, 1427–1433
40 Swain, J.L., Hines, J.J, Sabina, R.L., and Holmes, E.W. (1982) Accelerated repletion of ATP and GTP pools in postischemic canine myocardium using a precursor of purine *de novo* synthesis *Circ. Res.* **51**, 102–105